Macromolecules

Article

pubs.acs.org/Macromolecules

# Fabrication of Polymer Nanopeapods in the Nanopores of Anodic Aluminum Oxide Templates Using a Double-Solution Wetting Method

Jiun-Tai Chen,* Tzu-Hui Wei, Chun-Wei Chang, Hao-Wen Ko, Chien-Wei Chu, Mu-Huan Chi, and Chia-Chan Tsai

Department of Applied Chemistry, National Chiao Tung University, Hsinchu, Taiwan 30050

Supporting Information

**ABSTRACT:** Although one-dimensional polymer nanomaterials can be prepared by approaches such as the template method, the control over the morphologies of one-dimensional polymer nanomaterials containing multiple components is still a great challenge. In this work, we investigate the formation of polymer nanopeapods using a novel double-solution wetting method in the nanopores of anodic aluminum oxide (AAO) templates. A polystyrene (PS) solution in dimethylformamide (DMF) is first introduced into the nanopores of the AAO templates. Then a second polymer solution of poly(methyl methacrylate) (PMMA) in acetic acid is infiltrated into the nanopores. Because of the stronger interaction between acetic acid and aluminum oxide than that between DMF and aluminum oxide, the PMMA solution preferentially wets the pore walls of the templates and the PS solution is isolated in the center of the nanopores. After the evaporation of the solvent, peapod-like PS/PMMA nanostructures are obtained, where the shell and the core are composed of PMMA and PS, respectively. The compositions of the polymer nanopeapods are confirmed by removing PS or PMMA selectively. The formation mechanism of the nanostructures is related to the Rayleigh-instability-type transformation and further studied by changing experimental parameters such as the polymer concentration or the polymer molecular weight. This work not only provides a simple approach to prepare multicomponent polymer nanomaterials with controlled morphologies and sizes, but also contributes to a deeper understanding of polymer−solvent interactions in confined geometries.

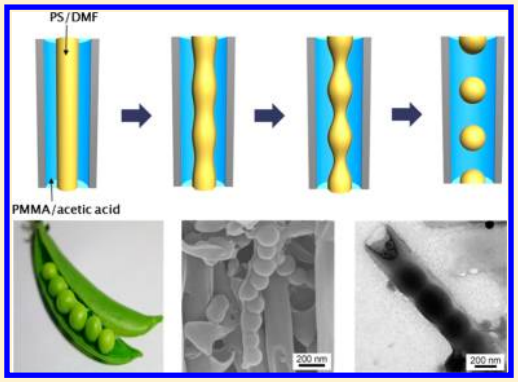


## INTRODUCTION

One-dimensional polymer nanomaterials have received much attention because of their unique properties and applications in areas such as sensors, filtration, tissue engineering, and photovoltaics.[1−4] One of the most common methods to prepare one-dimensional polymer nanomaterials is the template method.[5−7] Various one-dimensional polymer nanomaterials have been prepared using the template method, in which porous templates are used as scaffolds.[8] Polymer melts or solutions are first introduced into the nanopores of the templates. After the polymers are solidified in the nanopores, the templates can be removed selectively and the polymer nanomaterials are released. Because of the physical confinement of the nanopores, unusual morphologies of homopolymers or block copolymers, which are not accessible in the bulk, can be observed.[9−12]

Various materials have been explored as templates for the fabrication of one-dimensional nanomaterials, but anodic aluminum oxide (AAO) and ion-track-etched membranes are the most commonly used templates.[13,14] For ion-track membranes, which are usually made by polyester or polycarbonate films, the nanochannels are usually randomly distributed and the porosities are low.[15] AAO templates are prepared by electrochemical oxidation from aluminum. The main advantage of utilizing the AAO templates is their well-controlled pore sizes. Masuda et al. have pioneered a two-step anodization process to prepare well-ordered AAO templates with hexagonally packed nanopores of high pore densities.[16] The pore size, pore-to-pore distance, and pore length can be controlled by the anodization conditions.[17] Additionally, AAO templates can be dissolved easily after the fabrication of the nanomaterials using a selective etching solution such as a weak acid or a weak base.

Several wetting-based template methods have been developed for the fabrication of polymer nanomaterials, such as the melt method, the solvent-annealing method, and the solution method.[7,18,19] For the melt method, the polymer samples need to be heated above the glass transition temperatures ($T_g$) or the melting temperatures ($T_m$). Russell et al. investigated the wetting behavior of polystyrene (PS) melts in the nanopores of

Received: March 19, 2014
Revised: June 9, 2014
Published: July 16, 2014

AAO templates.[20] A transition from partial to complete wetting was observed, which is related to the spreading coefficient ($S$). The transition regions can be controlled by changing the polymer molecular weight or the annealing temperature.[20] Although the melt method is useful in making template-based polymer nanomaterials, it has the problem of thermal degradation, especially for samples which are heated above the melting temperatures of the polymers. Recently, solvent annealing−induced template wetting methods have also been developed.[21−23] Polymer chains wet the nanopores in the presence of solvent vapors. Depending on the type of solvent, polymer nanotubes or nanorods can be prepared due to the different wetting conditions (complete wetting or partial wetting).[23]

Other than the above two methods, the most versatile template-based wetting method is the solution wetting method.[18] The morphologies of the polymer nanostructures can be controlled by the polymer concentration, the solvent, or the molecular weight of the polymers.[24−28] Normally, polymer nanotubes are obtained using the solution wetting method. The wall thicknesses of the polymer nanotubes increase with the polymer concentrations. Wendorff et al. studied the effect of molecular weight on the formation of polystyrene nanostructures by wetting porous AAO templates with polystyrene solution.[29] They concluded that the formation of PS nanotubes, nanorods, or void structures are determined by the polymer molecular weight. Jin et al. also investigated the effect of interfacial interactions on the formation of PS nanostructures using different solvents.[24] They observed that the nanorod morphology can be obtained using solvents with preferential affinities to the pore wall of the AAO templates. Recently, we also studied the effect of adding nonsolvent (water) in the solution wetting method.[30−32] The stronger interaction between water and the alumina surface causes the polymer solution to be isolated in the center of the nanopores. Therefore, polymer nanospheres and nanorods instead of nanotubes can be formed after the wetting process.

Although different polymer nanomaterials can be fabricated using wetting-based template methods, it is still a great challenge to fabricate one-dimensional multicomponent polymer nanomaterials with controlled morphologies. The formation mechanisms of polymer nanomaterials containing two or more polymer components during the template wetting process are more complicated than those for single-component polymer nanomaterials.[33−35] For polymer blend films, it has been studied that there is an interplay between the phase separation and the wetting behavior.[36,37] The surface energy, thermodynamic interaction, and quenching depth are all critical to the formation of different morphologies in polymer blend films. Therefore, the formation processes of one-dimensional multicomponent polymer nanomaterails involve several interrelated factors, such as the chemistry of the pore wall, the size of the nanopore, the polymer molecular weight, the type of polymer, the type of solvent, the solution concentration, and the drying condition.[26,38−44] These factors are critical in controlling the sizes, the morphologies, and the properties of multicomponent polymer nanomaterials.

To further understand these effects, here we develop a double-solution wetting method to fabricate PS/PMMA nanomaterials (nanopeapods), in which PS nanospheres are embedded in the channels of PMMA nanotubes. A PS solution in dimethylformamide (DMF) is first introduced into the nanopores of the AAO templates via capillary force. Then a solution of PMMA in acetic acid is infiltrated into the nanopores. Because of the stronger interaction between the acetic acid solution to the AAO walls, a wetting layer of the PMMA in acetic acid can be formed on the pore walls of the AAO templates. Consequently, the PS solution in DMF is isolated in the center of the nanopores. After the evaporation of the solvent, PS/PMMA nanopeapods can be obtained.

The formation of these nanostructures is driven not only by the nonfavorable interaction between the polymer (PS) and the nonsolvent (acetic acid) but also by the confinement effect of the cylindrical nanopores of the templates. The compositions of the PS/PMMA nanopeapods are confirmed by selective removal processes of PS and PMMA using cyclohexane and acetic acid, respectively. The experimental parameters such as the polymer concentration or the polymer molecular weight are also changed to study their effects on the morphologies of PS/PMMA nanostructures. This study provides a unique and facile route to fabricate peapod-like PS/PMMA nanostructures with controlled morphologies and sizes. In addition to multicomponent polymer nanomaterials, this method can be applied to prepare organic/inorganic hybrid nanostructures by mixing polymer solutions with inorganic precursors.

## EXPERIMENTAL SECTION

**Materials.** Polystyrene (PS) with weight-average molecular weights ($M_w$) of 25, 35, 183, 490, and 934 kg/mol were purchased from Polymer Source and Sigma-Aldrich. Poly(methyl methacrylate) (PMMA) with a weight-average molecular weight ($M_w$) of 97 kg/mol was obtained from Sigma-Aldrich. Dimethylformamide (DMF) and sodium hydroxide (NaOH) were purchased from Tedia. Acetic acid was obtained from Sigma-Aldrich. Cyclohexane was obtained from J. T. Baker. Polycarbonate filters (VCTP, pore size: 0.1 $\mu$m) were obtained from Millipore. Wipers (Kimwipes) were purchased from Kimberly-Clark.

**Preparation of Synthesized AAO Templates.** The commercial AAO templates (pore diameter ∼150−400 nm, thickness ∼60 $\mu$m) were obtained from Whatman. The synthesized AAO templates were prepared using a two-step anodization method. In a typical anodization process, a high-purity aluminum sheet (99.99%, 0.5 mm thick) was degreased in acetone and rinsed by ethanol. Then the aluminum sheet was electropolished in a mixture of perchloric acid/ethanol at 4 °C. Subsequently, the aluminum sheet was anodized at 40 V in 0.3 M oxalic acid at 4 °C for 2 h. After the resultant aluminum oxide film was chemically etched in a phosphochromic acid solution for 4 h, a second anodization under the same conditions as for the first anodization was performed for different lengths of time, depending on the required length of the pores. The length of the pores is ∼40 $\mu$m when the second anodization is carried out for 7 h. The templates can be further pore-widened in phosphoric acid at 30 °C for 30 min, and the pore diameter can be increased to ∼50 nm.

**Fabrication of PMMA Nanotubes and PS Nanospheres.** To prepare PMMA nanotubes, an AAO template was first immersed in a 10 wt % PMMA ($M_w$ = 97 kg/mol) solution in acetic acid for 10 s. After the sample was taken out by a tweezer, the residual polymer solution on the outer surface of the AAO template was wiped by Kimwipes. After the sample was dried by a vacuum pump, the AAO template was dissolved selectively by 5 wt % NaOH(aq) to release the PMMA nanostructures.

To prepare PS nanospheres, an AAO template was first immersed in a 5 wt % PS ($M_w$ = 78.5 kg/mol) solution in DMF for 10 s. After the sample was taken out of the solution, the residual polymer solution on the outer surface of the AAO template was wiped by Kimwipes. Subsequently, the sample was dipped in acetic acid for 5 min. The sample was again taken out, and the surface was removed by Kimwipes. After the sample was dried by a vacuum pump, the AAO template was dissolved selectively by 5 wt % NaOH(aq) to release the PS nanostructures.

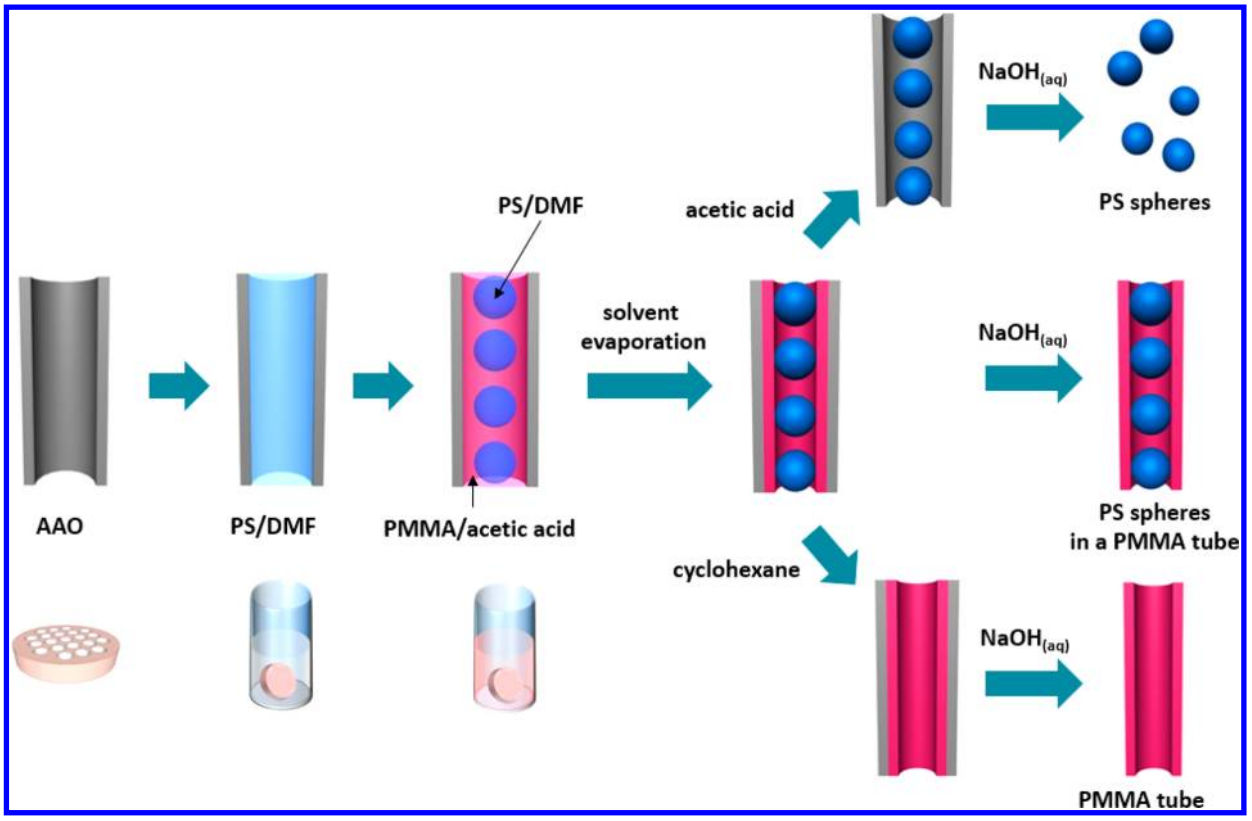


**Figure 1.** Schematic illustration of the experimental processes to prepare PS/PMMA nanopeapods. A PS solution in DMF is first introduced into the nanopores of an AAO template. Subsequently, the sample is dipped in a PMMA solution in acetic acid, resulting in the formation of peapod-like PS/PMMA nanostructures. PS nanospheres or PMMA nanotubes can be obtained by removing PS selectively using cyclohexane or removing PMMA selectively using acetic acid. AAO templates are dissolved by NaOH(aq) to release the polymer nanostructures.

**Fabrication of PS/PMMA Nanopeapods.** To fabricate PS/PMMA nanopeapods, PS and PMMA solutions with different concentrations were first prepared. A typical example to prepare PS/PMMA nanopeapods is shown as the following. An AAO template was immersed in a 5 wt % PS ($M_w$: 78.5 kg/mol) solution in DMF for 10 s. After the template was taken out of the PS solution, the residual solution outside the nanopores of the template was removed by Kimwipes. Subsequently, the sample was immersed in a 10 wt % PMMA ($M_w$: 97 kg/mol) solution in acetic acid for 5 min. The sample was again taken out of the PMMA solution, and the residual solution outside the nanopores of the templates was removed by Kimwipes. After the sample was dried by a vacuum pump, the AAO template was dissolved selectively by 5 wt % NaOH(aq) to release the PS/PMMA nanopeapods. Finally, the nanopeapods-containing solution was filtered using a polycarbonate filter while the sample was rinsed with DI water.

The morphology of the PS/PMMA nanopeapods can also be confirmed by the selective removing process. PMMA and PS can be removed selectively by acetic acid and cyclohexane, respectively. For example, a sample containing PS/PMMA nanopeapods was dipped in acetic acid for 24 h to remove PMMA and PS nanospheres can be obtained.

**Structure Analysis and Characterization.** The morphologies of the polymer nanostructures were examined by a JEOL JSM-7401F model scanning electron microscope (SEM) at an acceleration voltage of 5 kV. Before the SEM measurements, the samples were dried by a vacuum pump and coated with 4 nm of platinum. Bright-field transmission electron microscopy (TEM) measurements were also performed with a JEOL JEM-2100 TEM operating at an acceleration voltage of 200 kV. For TEM measurements, the samples were placed onto copper grids coated with Formvar or carbon.

## RESULTS AND DISCUSSION

In this work, AAO templates are used to fabricate PS/PMMA nanomaterials. The SEM images of commercial AAO templates are shown in Figure S1, and the average diameter of the nanopores of the templates is ~240 nm. We choose PS and PMMA, two commonly used polymers, to prepare the polymer nanopeapods. PMMA can have chemical bonding with the surface of the aluminum oxide wall and is used as the shell material of the polymer nanopeapods. PS only has a weaker interaction (physical absorption) with the AAO walls and is used as the core material.[45]

For making the PS/PMMA nanopeapods, the choice of solvents is critical and we select DMF and acetic acid as the solvents for PS and PMMA, respectively. DMF is intentionally used as the solvent for PS because it is a moderately good solvent for PS and miscible with acetic acid. The boiling point of DMF (~153 °C) is relatively high and can prevent the PS from solidification before the PMMA/acetic acid is introduced. For PMMA, acetic acid is used as the solvent because it is the nonsolvent for PS and has a stronger interaction to the alumina wall than DMF does. It is also crucial that acetic acid and DMF are miscible. Therefore, acetic acid can diffuse into the PS/DMF solution to promote the solidification of PS.

The experimental scheme for fabricating the polymer nanopeapods is shown in Figure 1. A PS (35 or 78.5 kg/mol) solution in DMF (5, 10, 20, 30 wt %) is first introduced into the nanopores of the AAO templates via capillary force. For nanopores wetted by a polymer solution, the maximum height ($h$) at which the polymer solution can reach via capillary


dx.doi.org/10.1021/ma500568j | Macromolecules 2014, 47, 5227−5235

force is inversely proportional to the radius of the nanopore of the template, given by Jurin's law[46]

$$h = 2\gamma(\cos\theta)/\rho g r \quad (1)$$

where $\gamma$ is the surface tension of the polymer solution, $\theta$ is the contact angle of the meniscus at the pore wall, $\rho$ is the density of the polymer solution, $g$ is gravity, and $r$ is the radius of the nanopore. Because of the small pore diameters (~150−400 nm), the maximum height at which the polymer solution can reach is higher than the length of the nanopores (~60 $\mu$m). The time for filling the nanopore is controlled by the viscosity of the polymer solution. In this work, the solution is drawn into the nanopores within a second because of the low viscosity of the polymer solution. After the nanopores are filled with the polymer solution via capillary force, the polymer solution outside the nanopores of the AAO templates is removed by wiping with Kimwipes. Without this process, a thick polymer film may be formed outside the nanopores of the AAO template after the evaporation of the polymer solution.

After the wiping process, the AAO template is dipped into the second polymer solution (PMMA in acetic acid) for 5 min. Then the AAO samples are taken out, and the polymer solution is wiped again by Kimwipes. Subsequently, the samples are dried by a vacuum pump for several hours. Polymer nanopeapods are formed in the nanopores of the AAO templates after the solvents are evaporated. In order to release the polymer nanostructures from the AAO templates, the samples are immersed into a 5 wt % NaOH solution for 30 min to remove the AAO templates selectively. Finally, the solutions are filtered by polycarbonate filter papers and washed with DI water. The polymer nanostructures are examined by both SEM and TEM.

Before fabricating the PS/PMMA nanopeapods, we first prepare PS nanospheres by dipping the AAO templates containing PS/DMF solution into acetic acid. The preferential interaction between acetic acid and the pore wall causes the formation of a wetting layer of acetic acid on the surface of the pore wall. As a result, the PS solution is isolated in the center of the nanopores. Driven by the Rayleigh-instability-type transformation, the PS solution undulates and breaks into spherical solution domains to reduce the interfacial area between the PS/DMF solution and acetic acid.[30] After the evaporation of the solvent, PS molecules precipitate and form nanospheres, as shown in Figure 2a,b. When acetic acid is introduced into the nanopores of the PS/DMF containing template, it is critical to make sure that the PS solution is not dried. Otherwise, PS nanotubes are formed because of the precipitation of the PS chains on the pore wall.

After we confirm that PS nanospheres can be prepared successfully by the nonsolvent effect of acetic acid, we then study the fabrication of PMMA nanotubes by wetting the AAO templates with PMMA/acetic acid solution. After the evaporation of acetic acid, the PMMA chains deposit on the pore wall, resulting in the formation of PMMA nanotubes, as shown in Figure 2c,d.[25] The lengths (~60 $\mu$m) and diameters (~150−400 nm) of the PMMA nanotubes are the same as those of the AAO nanopores. In Figure 2c, branched PMMA nanostructures can also be observed, indicating the branched part of the nanopores in the AAO template. The tubular nature of the PMMA nanostructures can be further confirmed by the TEM image. The diameter of the PMMA nanotube in Figure 2d is ~180 nm, and the wall thickness is ~10−20 nm. The nonuniform wall thickness may be caused by the fast evaporation process of the solvent and the nonuniform deposition of the PMMA chains. After the samples are dried by a vacuum pump, the morphologies of the PMMA nanotubes are maintained even after they are exposed to the aqueous NaOH solution.

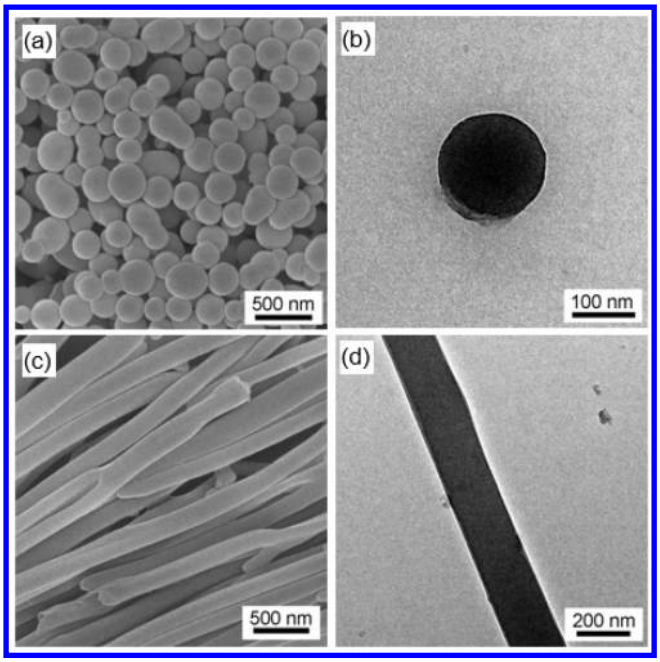


**Figure 2.** (a and b) SEM and TEM images of PS ($M_w$: 78.5 kg/mol) nanospheres. The PS nanospheres are prepared by dipping an AAO template in a 5 wt % PS solution in DMF, followed by immersing the sample into acetic acid. (c and d) SEM and TEM images of PMMA ($M_w$: 97 kg/mol) nanotubes. The PMMA nanotubes are prepared by dipping an AAO template in a 10 wt % PMMA solution in acetic acid.

After the feasibilities of the PS nanospheres and the PMMA nanotubes are confirmed, we then study the fabrication of the PS/PMMA nanopeapods. The PS/DMF solution is first introduced into the nanopores of an AAO template, followed by dipping the sample into the PMMA/acetic acid solution. The PS/DMF solution undergoes the Rayleigh-instability-type transformation and transforms into spherical solution domains. After the evaporation of the solvent, the PS nanospheres are deposited on the wall of PMMA nanotubes, as shown in Figure 3. Figure 3a shows the SEM image of the PS/PMMA nanopeapods, in which the smooth outer surface of the PMMA nanotubes can be observed. The sizes of the PS/PMMA nanopeapods correspond to the pore sizes of the AAO template (~150−400 nm). It has to be noted that the polymer nanostructures may be partially destroyed during the selective removal process of the AAO templates or during the filtration process. As a result, the PS nanospheres embedded in the PMMA nanotubes can be revealed, as shown in Figure 3b. The PS nanospheres are observed to stack on each other in PMMA nanotubes. The morphologies of the PS/PMMA nanopeapods can be confirmed further by the TEM image, as shown in Figure 3c, in which the PS nanospheres are embedded in the PMMA nanotubes.

In order to confirm the composition of the PS/PMMA nanopeapods, the selective removal technique is used. Acetic acid and cyclohexane are both chosen as the solvents for the selective removal process. Acetic acid is a nonsolvent for PS and can be used to dissolve PMMA selectively. On the contrary, cyclohexane is a nonsolvent for PMMA and can be used to


dx.doi.org/10.1021/ma500568j | Macromolecules 2014, 47, 5227−5235

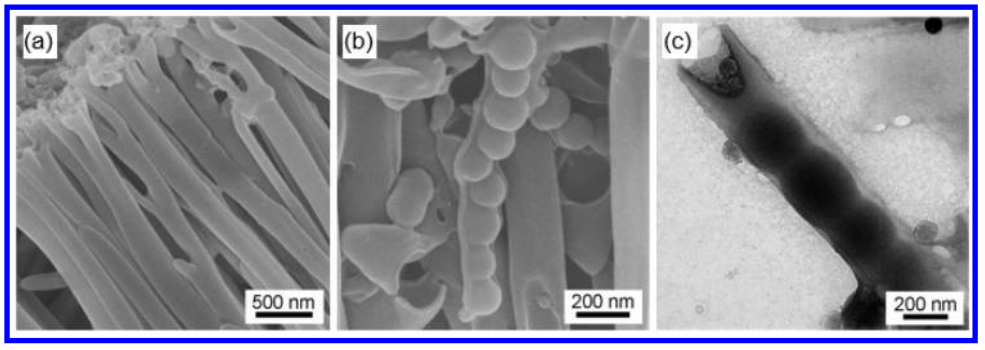


**Figure 3.** SEM (a and b) and TEM (c) images of peapod-like PS ($M_w$: 35 kg/mol) /PMMA ($M_w$: 97 kg/mol) nanostructures. The nanostructures are prepared by dipping AAO templates in PS solutions in DMF, followed by immersing the samples into 5 wt % PMMA solutions in acetic acid. The PS concentrations for the SEM (a and b) and TEM (c) samples are 1 and 5 wt %, respectively. In part b, some PS nanospheres are only covered partially by PMMA nanotubes, and the embedded PS nanospheres can be observed.

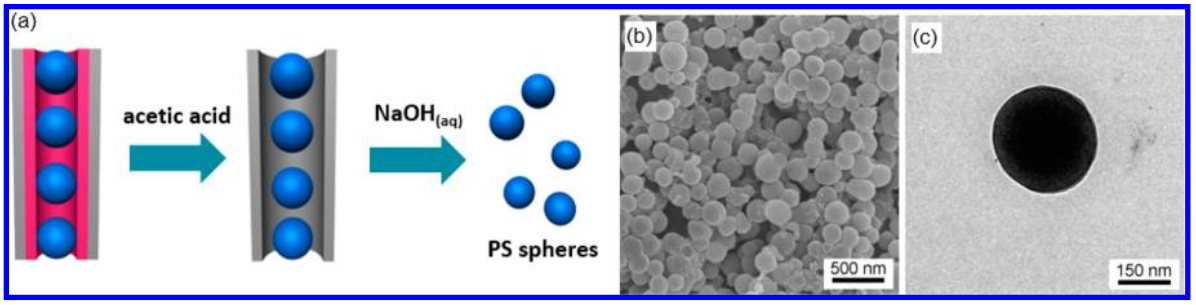


**Figure 4.** (a) Graphical illustration of the selective removal process to obtain PS nanospheres. (b and c) SEM and TEM images of PS ($M_w$: 35 kg/mol) nanospheres. The samples are first prepared by dipping AAO templates in 1 wt % PS solutions in DMF, followed by immersing the samples into 5 wt % PMMA ($M_w$: 97 kg/mol) solutions in acetic acid. After the samples are dried, PMMA is removed selectively by acetic acid. The AAO templates are then dissolved by NaOH(aq), and PS nanospheres can be obtained.

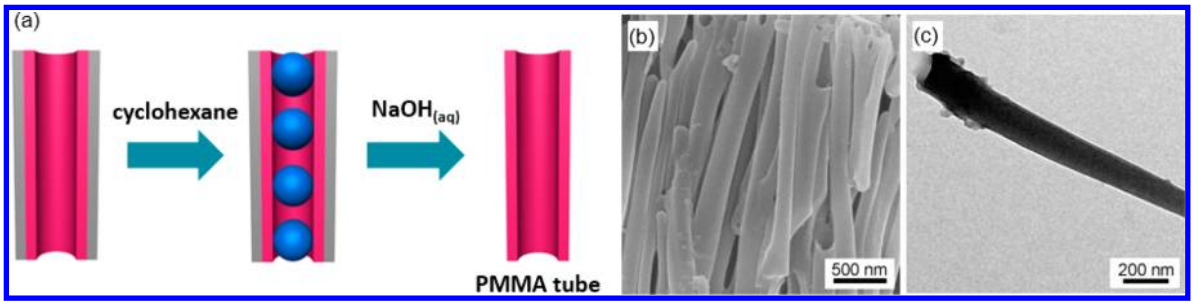


**Figure 5.** (a) Graphical illustration of the selective removal process to obtain PMMA nanotubes. (b and c) SEM and TEM images of PMMA ($M_w$: 97 kg/mol) nanotubes. The samples are first prepared by dipping AAO templates in 1 wt % PS ($M_w$: 35 kg/mol) solutions in DMF, followed by immersing the samples into 5 wt % PMMA solutions in acetic acid. After the samples are dried, PS is removed selectively by cyclohexane. The AAO templates are then dissolved by NaOH(aq), and PMMA nanotubes can be obtained.

dissolve PS selectively. Before performing the selective removal processes on the PS/PMMA nanopeapods, we have to confirm the selective removing abilities of these two solvents.

First, we examine whether cyclohexane is the nonsolvent for PMMA and the morphologies of the PMMA nanostructures are not affected by cyclohexane. Figure S2a shows the SEM image of PMMA ($M_w$: 97 kg/mol) nanotubes using the solution wetting method from a 5 wt % PMMA/acetic acid solution. After the PMMA nanotubes are immersed in cyclohexane for 24 h, the morphologies of the PMMA nanotubes are maintained, as shown in Figure S2b. Similarly, we examine whether acetic acid is the nonsolvent for PS and the morphologies of the PS nanostructures are not affected by acetic acid. Figure S2c shows the SEM image of PS ($M_w$: 35 kg/mol) nanotubes by using the solution wetting method from a 5 wt % PS/DMF solution. After the PS nanotubes are immersed in acetic acid for 24 h, the morphologies of PS nanotubes are maintained, as shown in Figure S 2d.

The experimental process to remove selectively the PMMA nanotubes in the PS/PMMA nanopeapods and to obtain PS nanospheres is illustrated in Figure 4a. The PS/PMMA nanopeapods are first prepared by using 1 wt % PS/DMF solution and 5 wt % PMMA/acetic acid solution. After the PS/PMMA nanostructures are solidified in the AAO nanopores, the sample is dipped into acetic acid to remove selectively the PMMA nanotubes. After the removal process, PS nanospheres can be obtained, as shown in the SEM and TEM images (Figure 4b,c). These results confirm that the core material of the polymer nanopeapods is composed of PS.

The experimental process to remove selectively the PS nanospheres in the PS/PMMA nanopeapods and to obtain the PMMA nanotubes is illustrated in Figure 5a. As shown in the


dx.doi.org/10.1021/ma500568j | *Macromolecules* 2014, 47, 5227−5235

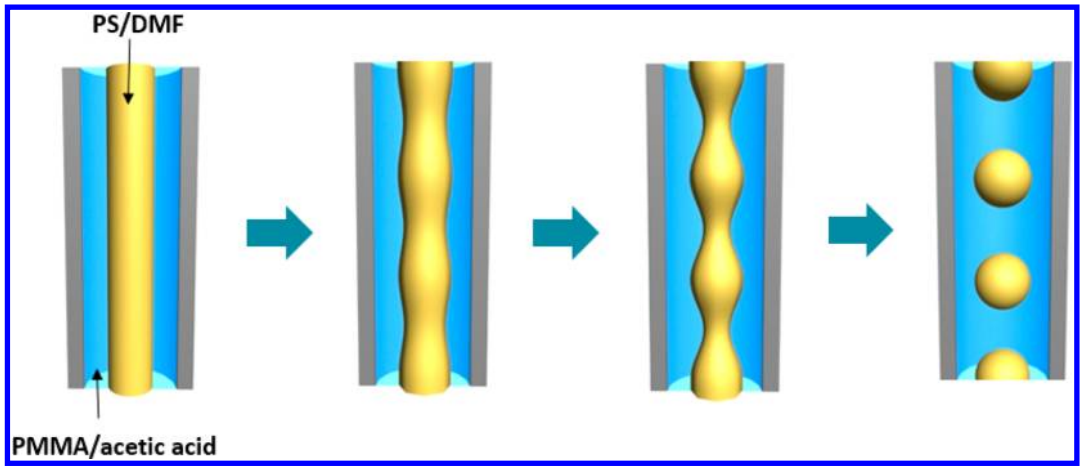


**Figure 6.** Proposed model of the formation mechanism of polymer nanostructures by using the double-solution wetting method. Because of the stronger interaction between acetic acid and aluminum oxide than that between DMF and aluminum oxide, the PMMA/acetic acid solution can preferentially wet the pore walls of the templates. The PS/DMF solution is isolated in the center of the nanopores. The PS/DMF solution cylinder breaks into droplets, driven by the Rayleigh-instability-type transformation to reduce the interfacial energy between two solution domains. After the evaporation of the solvents, peapod-like PS/PMMA composite nanostructures are obtained, where the shell and the core are composed of PMMA and PS, respectively.

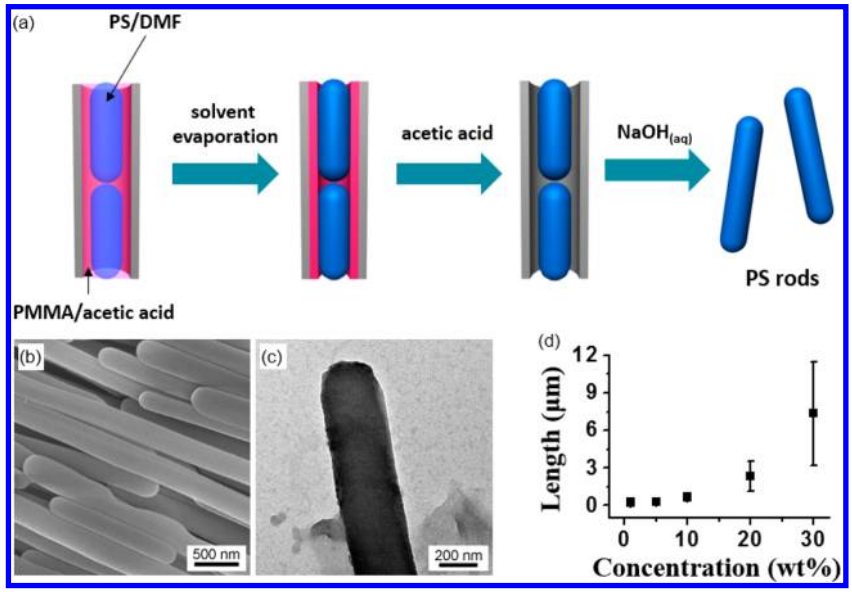


**Figure 7.** (a) Graphical illustration of the experimental process to prepare PS/PMMA nanostructures and PS nanorods using PS/DMF solutions with higher concentrations. (b) SEM image of PS ($M_w$: 78.5 kg/mol) nanorods using a 30 wt % PS/DMF solution. (c) TEM image of a PS ($M_w$: 78.5 kg/mol)/PMMA ($M_w$: 97 kg/mol) nanostructure using a 30 wt % PS/DMF solution. (d) Plot of the length of the PS ($M_w$: 78.5 kg/mol) nanorods versus the concentration of the PS/DMF solution. The concentration of the PMMA solution is 10 wt %.

SEM and TEM images (Figure 5b,c), the PS nanospheres can be removed successfully by cyclohexane and PMMA nanotubes can be obtained. Both the selective removal processes confirm that the shell material of the PS/PMMA nanopeapods is PMMA and the core material is PS.

On the basis of the experimental results, a simple model is proposed to explain the formation mechanism of the PS/PMMA nanopeapods, as shown in Figure 6. At first, nanopores of an AAO template are filled with a solution of PS/DMF. Then the solution of PMMA/acetic acid is introduced into the nanopores. Because of the stronger interaction between acetic acid and the AAO wall than that between DMF and the AAO wall, the PS/DMF solution is isolated in the center of the AAO nanopores. The PS/DMF solution cylinder breaks into droplets, driven by the Rayleigh-instability-type transformation to reduce the interfacial energy between two solution domains.[47,48] After the evaporation of the solvents, peapod-like PS/PMMA composite nanostructures are obtained, where the shell and the core are composed of PMMA and PS, respectively.

The formation process of the PS/PMMA nanostructures is related to the Rayleigh-instability-type transformation. The Rayleigh-instability is commonly seen in our daily life. For example, when water is coming out of the faucet, the water cylinder breaks into spherical water droplets at the end of the water cylinder. Joseph Plateau was the first to study the Rayleigh instability.[47] He showed that the free surface of a liquid cylinder distorts and disintegrates into a chain of droplets to reduce the surface energy. When the undulation wavelength ($\lambda$) is larger than the circumference of the cylinder ($2\pi R_0$), the


dx.doi.org/10.1021/ma500568j | Macromolecules 2014, 47, 5227−5235

surface area decreases until the cylindrical liquid cylinder breaks into spherical droplets.

Later, Rayleigh demonstrated that the wavelength of the distortion and the size of the droplets are determined by the fastest distortion mode.[43] Nichols and Mullins extended the Rayleigh's theory to solid cylinders.[49] They studied the mass transport of solid cylinders by surface diffusion or solid diffusion. The perturbed surface can be expressed by the following equation

$$r = R_0 + \delta \sin(2\pi/\lambda)z \quad (2)$$

where $\delta$ is the amplitude of the undulation, $\lambda$ is the undulation wavelength, and $z$ is along the cylinder axis. Once the wavelength $\lambda > 2\pi R_0$, the amplitude of the surface increases spontaneously. The perturbation with the maximum growth rate determines the dominant wavelength $\lambda_m = 2\pi\sqrt{2}R_0 = 8.89R_0$. With time, the amplitude of the perturbation increases at the maximum growth rate and finally breaks up into a line of spheres.

In our experiments, the cylindrical PS/DMF solution breaks into spherical solution domains to reduce the interfacial areas between the PS/DMF solution and the surrounding PMMA/acetic acid solution, similar to the phenomenon of the Rayleigh instability. Later, acetic acid may diffuse into the PS/DMF solution droplets and cause the PS molecules to precipitate, resulting in the formation of PS nanospheres. It has to be noted that this model is a simplified view of the transformation process because the breakup of the PS/DMF solution and the diffusion of the acetic acid may occur simultaneously.

To study the morphologies of the PS/PMMA nanopeapods further, we also change the concentrations of the PS/DMF solutions and the PMMA/acetic acid solutions. The PS nanospheres demonstrated above are from PS/DMF solutions with the concentration of 1 and 5 wt %. Figure 7a shows the graphical illustration of the experimental process to prepare PS nanorods using PS/DMF solutions with higher concentrations. At higher concentrations, the PS/DMF solutions break into longer solution domains and PS nanorods are formed after the evaporation of the solvents. For example, PS ($M_w$: 78.5 kg/mol) nanorods with an average length of ~8 $\mu$m can be obtained using a 30 wt % PS/DMF solution, as shown in the SEM and TEM images (Figure 7b,c). The PS nanostructures obtained using other concentrations are displayed in Figure S3 in the Supporting Information. The highest PS concentration we use is 30 wt % because of the processing difficulties at high solution viscosities. When the PS concentration is higher than 20 wt %, it is difficult to measure the lengths of some nanorods correctly due to the limitation of the scanning area in the SEM measurement, causing larger standard deviations at higher concentrations. Figure 7d shows the plot of the length of the PS ($M_w$: 78.5 kg/mol) nanorods versus the concentration of the PS/DMF solution, where the concentrations of the PMMA solutions are fixed at 10 wt %. The length of the PS nanorods increases with the PS/DMF concentrations, as expected.

To understand the formation mechanism of the polymer nanopeapods further, we also study the intermediate morphologies of the nanostructures by changing the molecular weight of PS. Using a polymer with different molecular weights, the viscosity of the polymer solution can be controlled. Under the same polymer concentration, the polymers with a higher molecular weight can cause stronger entanglements of the polymer chains, resulting in a higher solution viscosity.

For viscoelastic materials, the viscosity can resist the breakup of the materials driven by the Rayleigh instability.[50−52] The breakup of viscoelastic materials is related to the characteristic time by the following equation

$$\tau_m = \eta R_0/\sigma \quad (3)$$

where $\tau_m$ is the characteristic time for the fastest growing mode in the Rayleigh instability, $\eta$ is the viscosity of the viscoelastic material, $R_0$ is the radius of the liquid cylinder, and $\sigma$ is the interfacial tension between the materials and the surrounding medium.[11,50] From eq 3, the characteristic time of the Rayleigh-instability-type transformation is proportional to the viscosity of the polymer solution. Therefore, longer transformation times are required for polymers with higher molecular weights to form spherical domains. If the samples are dried before the transformation processes are completed, the intermediate undulated structures can be observed.

Figure 8 shows the PS nanostructures using PS with different molecular weight ($M_w$ = 25, 183, 490, and 934 kg/mol). The concentrations of the PS/DMF solutions and the PMMA/acetic acid solutions are fixed at 5 and 10 wt %, respectively. After the PMMA nanotubes are removed selectively by acetic acid, the PS nanostructures can be examined. For PS with lower molecular weights (25 or 183 kg/mol), the characteristic times for the Rayleigh-instability-type transformation are shorter because of the lower solution viscosities. Therefore, the transformation processes can be completed before the solvents are evaporated, resulting in the formation of PS nanospheres (Figure 8a,b). For PS with higher molecular weights (490 and 934 kg/mol), however, the transformation processes are not completed, and undulated PS nanostructures can be obtained, as shown in Figure 8c,d.

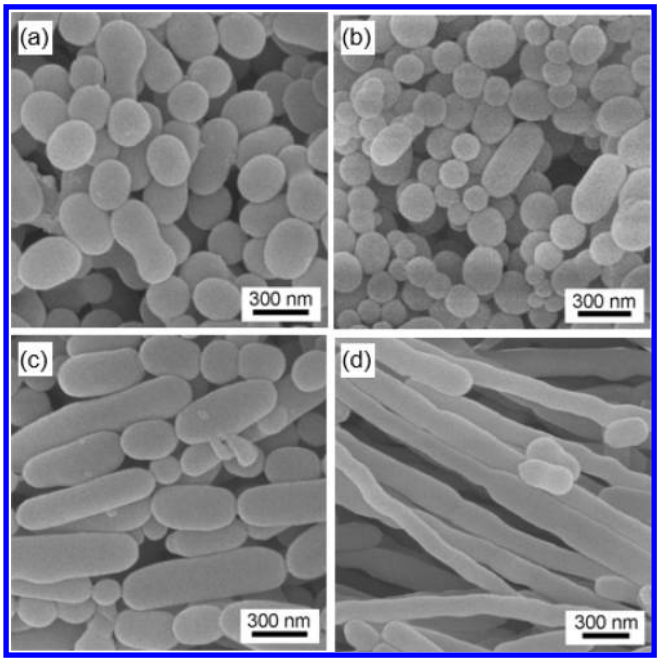


**Figure 8.** SEM images of PS nanostructures using PS with different molecular weights: (a) 25, (b) 183, (c) 490, and (d) 934 kg/mol. The samples are prepared by dipping AAO templates in 5 wt % PS solutions in DMF, followed by immersing the samples into 10 wt % PMMA ($M_w$: 97 kg/mol) solutions in acetic acid. After the samples are dried, PMMA is removed selectively by acetic acid and PS nanostructures can be obtained.


dx.doi.org/10.1021/ma500568j | Macromolecules 2014, 47, 5227−5235

Even though the experimental results can be explained by the simple model shown in Figure 6, the real formation mechanism of the polymer nanopeapods using the double-solution wetting method is considered to be more complicated. Acetic acid is soluble in DMF, so the interfaces between the PS/DMF and the PMMA/acetic acid solutions are not well-defined. If acetic acid diffuses into the PS/DMF solution by the Fickian diffusion, broad interfaces are expected.[53] If the PS/DMF solution is partially dried, acetic acid may diffuse into the concentrated PS/DMF solution by the non-Fickian diffusion (case II).[54] In the case of the non-Fickian diffusion, the diffusion constant is also a function of the concentration of the polymer solution, and a sharp interface may be formed.[55] Furthermore, the rate of precipitation of the PS is affected by the diffusion rate of acetic acid. To address these issues, a more sophisticated model reflecting the real formation process of the polymer nanopeapods may be necessary to develop in the future.

The data shown above are obtained using commercial AAO templates with pore sizes ~100−400 nm. The broad pore sizes can actually give us some advantages. For example, nanostructures with different diameters can be observed on a single sample using the commercial AAO templates, which is beneficial to demonstrate the generality of this strategy. In addition to the commercial templates, we also synthesize AAO templates by electrochemical oxidation of aluminum sheets in oxalic acid. The pore diameter can be further increased to ~50 nm by dipping the template in phosphoric acid at 30 °C for 30 min. The SEM images of the synthesized AAO templates (pore diameters ~50 nm) are shown in Figure S4 in the Supporting Information.

With the synthesized AAO templates, experiments are conducted to prepare PS/PMMA nanopeapods and the results are shown in Figure S5 in the Supporting Information. Similar to the results from the commercial AAO templates (pore diameter ~150−400 nm), PS/PMMA nanopeapods with smaller sizes can be obtained from the synthesized AAO templates (pore diameter ~50 nm). As shown in the SEM and TEM images (Figure S5a,c), the outer diameters of the nanopeapods (~50 nm) agree well with the pore diameters of the synthesized AAO templates. After the outer PMMA shell is selectively removed by acetic acid, PS spheres with the diameters ~30−50 nm can be obtained. The experimental data successfully demonstrate that polymer nanopeapods with smaller sizes can be obtained using the synthesized AAO templates with smaller pore diameters.

## CONCLUSION

We demonstrate the preparation of polymer nanopeapods using the double solution wetting method. The preferential interaction of the PMMA solution in acetic acid to the aluminum oxide walls causes the PS solution in DMF to be isolated in the center of nanopores of the AAO templates. PS nanospheres are formed after the breakup of PS/DMF solution, driven by the Rayleigh-instability-type transformation, and the evaporation of the solvent. PS nanorods instead of nanospheres can be formed by increasing the concentrations of the PS/DMF solutions. This study demonstrates that the sizes and morphologies of polymer composite nanomaterials can be easily controlled by manipulating the polymer−solvent, the solvent−alumina, and the polymer−alumina interactions. Possible future works include the fabrication of conjugated polymer or block copolymer nanostructures using the double solution wetting method. Organic/inorganic can also be prepared by mixing inorganic precursors with polymer solutions.

## ASSOCIATED CONTENT

### Supporting Information

The SEM images of the AAO templates and polymer nanomaterials. This material is available free of charge via the Internet at http://pubs.acs.org.

## AUTHOR INFORMATION

### Corresponding Author

*(J.-T.C.) E-mail: jtchen@mail.nctu.edu.tw.

### Notes

The authors declare no competing financial interest.

## ACKNOWLEDGMENTS

This work was supported by the Ministry of Science and Technology of the Republic of China.

## REFERENCES

(1) Jang, J.; Springer, V. Conducting polymer nanomaterials and their applications. In *Emissive Materials: Nanomaterials*; Springer-Verlag Berlin: Berlin, 2006; Vol. *199*, pp 189−259.
(2) Aleshin, A. N. *Adv. Mater.* **2006**, *18* (1), 17−27.
(3) Pham, Q. P.; Sharma, U.; Mikos, A. G. *Tissue Eng.* **2006**, *12* (5), 1197−1211.
(4) Chen, J. T.; Hsu, C. S. *Polym. Chem.* **2011**, *2* (12), 2707−2722.
(5) Martin, C. R. *Acc. Chem. Res.* **1995**, *28* (2), 61−68.
(6) Steinhart, M. Supramolecular Organization of Polymeric Materials in Nanoporous Hard Templates. In *Self-Assembled Nanomaterials Ii: Nanotubes*, Shimizu, T., Ed. Springer-Verlag Berlin: Berlin, 2008; Vol. *220*, pp 123−187.
(7) Martin, J.; Maiz, J.; Sacristan, J.; Mijangos, C. *Polymer* **2012**, *53* (6), 1149−1166.
(8) Hurst, S. J.; Payne, E. K.; Qin, L. D.; Mirkin, C. A. *Angew. Chem., Int. Ed.* **2006**, *45* (17), 2672−2692.
(9) Shi, A. C.; Li, B. H. *Soft Matter* **2013**, *9* (5), 1398−1413.
(10) Dobriyal, P.; Xiang, H. Q.; Kazuyuki, M.; Chen, J. T.; Jinnai, H.; Russell, T. P. *Macromolecules* **2009**, *42* (22), 9082−9088.
(11) Chen, J. T.; Zhang, M. F.; Russell, T. P. *Nano Lett.* **2007**, *7* (1), 183−187.
(12) Blaszczyk-Lezak, I.; Hernandez, M.; Mijangos, C. *Macromolecules* **2013**, *46* (12), 4995−5002.
(13) Huczko, A. *Appl. Phys. A: Mater. Sci. Process.* **2000**, *70* (4), 365−376.
(14) Jani, A. M. M.; Losic, D.; Voelcker, N. H. *Prog. Mater. Sci.* **2013**, *58* (5), 636−704.
(15) Apel, P. *Radiat. Meas.* **2001**, *34* (1−6), 559−566.
(16) Masuda, H.; Fukuda, K. *Science* **1995**, *268* (5216), 1466−1468.
(17) Li, A. P.; Muller, F.; Birner, A.; Nielsch, K.; Gosele, U. *J. Appl. Phys.* **1998**, *84* (11), 6023−6026.
(18) Cepak, V. M.; Martin, C. R. *Chem. Mater.* **1999**, *11* (5), 1363−1367.
(19) Steinhart, M.; Wendorff, J. H.; Greiner, A.; Wehrspohn, R. B.; Nielsch, K.; Schilling, J.; Choi, J.; Gosele, U. *Science* **2002**, *296* (5575), 1997−1997.
(20) Zhang, M. F.; Dobriyal, P.; Chen, J. T.; Russell, T. P.; Olmo, J.; Merry, A. *Nano Lett.* **2006**, *6* (5), 1075−1079.
(21) Wang, T. C.; Hsueh, H. Y.; Ho, R. M. *Chem. Mater.* **2010**, *22* (16), 4642−4651.
(22) Mei, S. L.; Feng, X. D.; Jin, Z. X. *Soft Matter* **2013**, *9* (3), 945−951.
(23) Chen, J. T.; Lee, C. W.; Chi, M. H.; Yao, I. C. *Macromol. Rapid Commun.* **2013**, *34* (4), 348−354.
(24) Feng, X. D.; Jin, Z. X. *Macromolecules* **2009**, *42* (3), 569−572.

(25) Chen, J. T.; Shin, K.; Leiston-Belanger, J. M.; Zhang, M. F.; Russell, T. P. *Adv. Funct. Mater.* **2006**, *16* (11), 1476−1480.
(26) Chen, J. T.; Zhang, M. F.; Yang, L.; Collins, M.; Parks, J.; Avallone, A.; Russell, T. P. *J. Polym. Sci., Part B: Polym. Phys.* **2007**, *45* (20), 2912−2917.
(27) Pasquali, M.; Liang, J.; Shivkumar, S. *Nanotechnology* **2011**, *22* (37), 375605.
(28) Wei, T. H.; Chi, M. H.; Tsai, C. C.; Ko, H. W.; Chen, J. T. *Langmuir* **2013**, *29* (32), 9972−9978.
(29) Schlitt, S.; Greiner, A.; Wendorff, J. H. *Macromolecules* **2008**, *41* (9), 3228−3234.
(30) Lee, C. W.; Wei, T. H.; Chang, C. W.; Chen, J. T. *Macromol. Rapid Commun.* **2012**, *33* (16), 1381−1387.
(31) Chi, M. H.; Kao, Y. H.; Wei, T. H.; Lee, C. W.; Chen, J. T. *Nanoscale* **2014**, *6* (3), 1340−1346.
(32) Huang, Y. C.; Fan, P. W.; Lee, C. W.; Chu, C. W.; Tsai, C. C.; Chen, J. T. *ACS Appl. Mater. Interfaces* **2013**, *5* (8), 3134−3142.
(33) Jin, S.; Lee, Y.; Jeon, S. M.; Sohn, B. H.; Chae, W. S.; Lee, J. K. *J. Mater. Chem.* **2012**, *22* (44), 23368−23373.
(34) Kriha, O.; Zhao, L. L.; Pippel, E.; Gosele, U.; Wehrspohn, R. B.; Wendorff, J. H.; Steinhart, M.; Greiner, A. *Adv. Funct. Mater.* **2007**, *17* (8), 1327−1332.
(35) Chen, D.; Chen, J. T.; Glogowski, E.; Emrick, T.; Russell, T. P. *Macromol. Rapid Commun.* **2009**, *30* (4−5), 377−383.
(36) Geoghegan, M.; Ermer, H.; Jungst, G.; Krausch, G.; Brenn, R. *Phys. Rev. E* **2000**, *62* (1), 940−950.
(37) Geoghegan, M.; Krausch, G. *Prog. Polym. Sci.* **2003**, *28* (2), 261−302.
(38) Wang, Y.; Tong, L.; Steinhart, M. *ACS Nano* **2011**, *5* (3), 1928−1938.
(39) Chen, D.; Park, S.; Chen, J. T.; Redston, E.; Russell, T. P. *ACS Nano* **2009**, *3* (9), 2827−2833.
(40) Feng, X. D.; Mei, S. L.; Jin, Z. X. *Langmuir* **2011**, *27* (23), 14240−14247.
(41) Chen, J. T.; Chen, D.; Russell, T. P. *Langmuir* **2009**, *25* (8), 4331−4335.
(42) Chen, D.; Zhao, W.; Wei, D. G.; Russell, T. P. *Macromolecules* **2011**, *44* (20), 8020−8027.
(43) Han, G. Q.; Liu, Y. H.; Luo, J. B.; Lu, X. C. *J. Nanosci. Nanotechnol.* **2011**, *11* (11), 10240−10246.
(44) Wu, H.; Su, Z. H.; Takahara, A. *Polym. J.* **2011**, *43* (7), 600−605.
(45) Nunnery, G. A.; Jacob, K. I.; Tannenbaum, R. *Langmuir* **2012**, *28* (42), 14960−14967.
(46) de Gennes, P. G.; Brochard-Wyart, F.; Quere, D. *Capillarity and Wetting Phenomena*; Springer: New York, 2004.
(47) Plateau, J. *Transl. Annu. Rep. Smithsonian Inst.* **1873**, 1863−1866.
(48) Rayleigh, L. *Proc. London Math. Soc.* **1878**, *10*, 4−13.
(49) Nichols, F. A.; Mullins, W. W. *Trans. Met. Soc. AIME* **1965**, *233*, 1840−1848.
(50) Edmond, K. V.; Schofield, A. B.; Marquez, M.; Rothstein, J. P.; Dinsmore, A. D. *Langmuir* **2006**, *22* (21), 9052−9056.
(51) Fan, P. W.; Chen, W. L.; Lee, T. H.; Chen, J. T. *Macromol. Rapid Commun.* **2012**, *33* (4), 343−349.
(52) Fan, P. W.; Chen, W. L.; Lee, T. H.; Chiu, Y. J.; Chen, J. T. *Macromolecules* **2012**, *45* (14), 5816−5822.
(53) Masaro, L.; Zhu, X. X. *Prog. Polym. Sci.* **1999**, *24* (5), 731−775.
(54) Weisenberger, L. A.; Koenig, J. L. *Macromolecules* **1990**, *23* (9), 2445−2453.
(55) Sanopoulou, M.; Stamatialis, D. F.; Petropoulos, J. H. *Macromolecules* **2002**, *35* (3), 1012−1020.